JOHN JAEGER MEMORIAL LECTURE

Some Plasticity Solutions Relevant to the Bearing Capacity of Rock and Fissured Clay

E. H. DAVIS, BSc, FIE Aust, FAA
Professor of Civil Engineering, University of Sydney

Opening remarks

Before giving my lecture I should like to record how honoured I feel in receiving the John Jaeger Memorial Medal. I accept it not only as recognition of my own work but particularly in recognition of the work of the whole Geomechanics group at the University of Sydney; Dr Poulos, Dr Booker, Dr Brown, Mr Pells and an exceptionally gifted series of research students both past and present. We have all been very happy working together and I am sure will continue so. I am also very pleased that this medal is named after Professor Jaeger. He was a most distinguished Australian scientist and he was a true academic in that all his work, both theoretical and experimental was of the highest quality. His textbooks are of lasting value and a joy to refer to. My only regret is that we in Engineering Geomechanics didn't have as much contact with him as we ought to have had. It was our fault not his, and we could have benefitted greatly. So I am proud to receive the first medal and proud that it bears the name of John Jaeger.

Introduction

The main purpose of this lecture is to examine the truth of the following statement:

> "The maximum load capacity of a mass of soil or rock is not uniquely dependent on the strength of an element of the material."

Although, when put baldly like that, most of us would agree with this statement, we frequently continue to reply on conventional stability analysis which only requires the input of one pair of strength parameters of the material - c and ϕ. That this may lead to an unreliable estimate of the overall stability of a mass of soil or rock arises from two main factors.

a) Semi-brittle behaviour - dense granular soils, over consolidated clays and virtually all rocks have a peak strength. Beyond this peak, further plastic straining produces a strain softening with loss of strength until a constant residual or ultimate strength is reached. The ratio of peak to residual strength (sensitivity or brittleness ratio) is obviously a major parameter in determining the extent to which the semi-brittle behaviour affects the overall stability of a mass of such material. But the ratio of softening to the elastic modulus, what may be termed the softening ratio, clearly may also play an important role, since it will determine the extent to which some zones in the mass have already been strained well beyond the peak by the time the mass reaches its maximum load capacity. This maximum occurs when sufficient additional zones of the mass reach peak strength to allow unrestricted plastic flow so that collapse follows. Is it too optimistic to use the undisturbed strength of a sensitive clay, or the peak ϕ of a dense sand to predict the bearing capacity of foundations on such soils? Or is it too pessimistic to use the fully remoulded strength of the clay or ϕ_{cv} of the sand?

b) Defects - some soil and most rock masses contain defects (joints, cracks, bedding planes, fissures in clay etc) which have lower strength properties (c and/or ϕ) than the intact material. This is recognised in rock mechanics, sometimes to the exclusion of consideration of the possible contribution of the intact strength to the overall mass stability, but is not often allowed for in soil mechanics. If the sets of defects are reasonably constant in orientation and closely spaced the mass can be considered to be homogeneous but anisotropic, the properties of this composite material being determined by the defect strength, the intact strength and the orientation of the defect sets. Under what circumstances do the defects have a negligible weakening effect on say the bearing capacity of the mass or under what circumstances does their strength dominate?

This lecture is concerned with examining the theoretical effects of semi-brittle behaviour and of the presence of defects on the stability of soil and rock masses. For simplicity, attention is restricted to surface bearing capacity of the mass under plane strain conditions, and, for the most part, ignoring the effect of density of the material. Attention is also restricted to failure of the mass due to a monotonically increasing load or single load application but an aside on the subject of incremental failure for cyclic loading is worth making.

Cyclic loading - an aside

In recent years there has been much attention paid to the stability of foundations under cyclic loading, this being an important aspect of the design of off-shore structures. Most of the research work in this area has been concerned with loss of strength of the soil resulting from degration of the particles, build up of pore water pressures, or other 'fatigue' effects of cyclic stressing. It is less commonly recognised that, even if the strength of the soil is not reduced by cyclic stressing, the foundation and soil mass system can fail by incremental plastic collapse although all combinations of load applied to the foundations within the repeated cycle are less than those required to cause single or monotonic load collapse. On the other hand, the existence of 'shakedown' limits for cyclic loading has long been recongised in relation to structural frames.

The shakedown of surface strip footings under combined loads has recently been considered by Pande et al (1980) and Aboustit and Reddy (1980). The results of some recent theoretical studies at the University of Sydney (Swane 1980) on the shakedown limit for cyclic lateral loading of a pile in clay, the strength of which is unaffected by cyclic stressing, are given in figures 1 and 2. The combination of moment and horizontal load to produce collapse under a single or monotonically increasing loading are shown as a large full-line loop. In contrast, the combination of cyclic load, about a mean load of $M = M_o$ and $H = H_o = O$, to produce incremental collapse are shown as the smaller dashed-line loop. Changing from a rigid pile (Fig.1) to a flexible pile (Fig.2) does not alter the large full-line loop but reduces the cyclic load capacity further. It should be pointed out that, for material with strength properties unaffected by cyclic stressing, the single load capacity of the system remains unaffected by cyclic loading. If, after any number of load cycles within the large full-line loop, cycling is stopped and the loading is increased monotonically along any M/H path, plastic collapse will still only occur when the loading path intersects the large full-line loop.

The remainder of this lecture is concerned with collapse under single or monotonic loading.

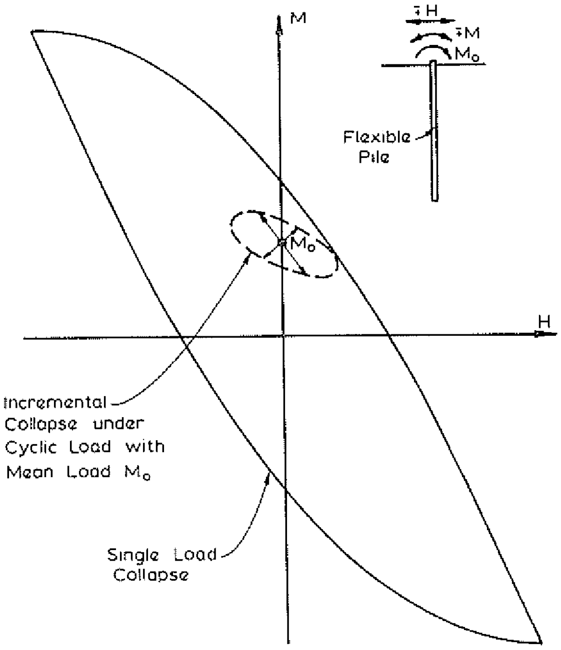

FIG 2 SHAKEDOWN FOR LATERALLY LOADED FLEXIBLE PILE (Swane,1980)

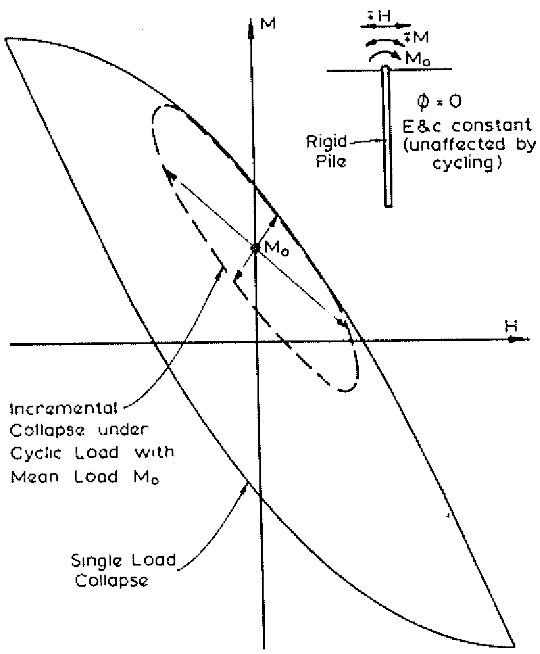

FIG 1 SHAKEDOWN FOR LATERALLY LOADED RIGID PILE (Swane,1980)

Strain Softening

The effect of strain softening on the bearing capacity of a strip footing on dense sand is well illustrated by the results of model footing tests conducted by Kirkpatrick and Uzuner (Kirkpatrick 1977) as shown in fig.3. In order to include the wide range of theoretical bearing capacities the load is plotted to a logarithmic scale in this figure. These theoretical values for a rough footing have been calculated from plasticity theory for a simple frictional plastic with no softening behaviour (Davis and Booker 1971). It can be seen that, although the experimental results show a peak followed by a lower ultimate bearing capacity, the ratio of the two values is much closer to unity than the ratio of the theoretical bearing capacities for $\phi = \phi_{peak}$, and $\phi = \phi_{cv}$ using the values of ϕ from plane strain testing. The experimental peak is only about a quarter of the theoretical value from simple plasticity theory using $\phi = \phi_{peak}$ whereas the ultimate experimental value is close to that given by the theory using $\phi = \phi_{cv}$. The situation is confused by the common but inappropriate use of triaxial compression values of ϕ for plane strain stability problems. In this case, this would lead fortuitously to closer agreement between the simple theory and experiment. It may be further commented that, although it is common experience that plane strain values of ϕ are higher than triaxial values, the difference in Kirkpatrick and Uzuner's tests is surprisingly high.

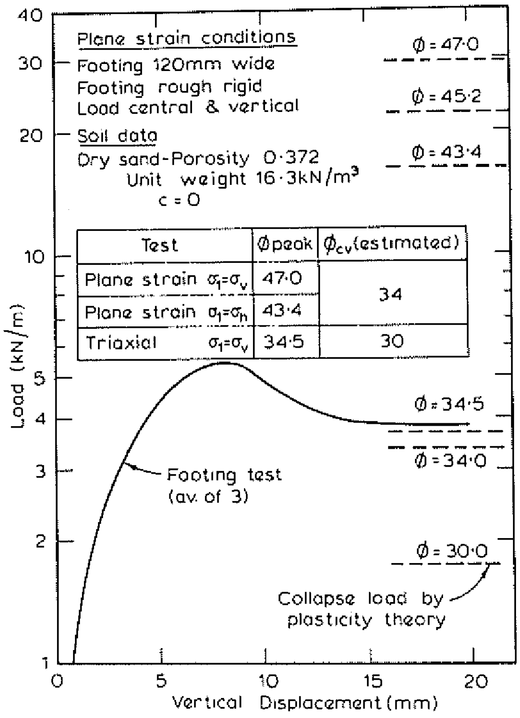

FIG 3 MODEL FOOTING TEST ON SAND
(Kirkpatrick and Uzuner, 1977)

In principle, it should be possible to examine theoretically the effect of strain softening by incorporating appropriate strain softening constitutive laws into a numerical analysis such as a finite element method. In practice there are problems of numerical accuracy, particularly those associated with bifurcation - the development of narrowing zones of increasing intensity of plastic shear strain in parts of the mass which have passed the peak strength. It is therefore useful for bearing capacity studies to consider a simple theoretical model which approximately reproduces the main features of the manner in which a mass of material supports a surface footing but of itself can be analysed exactly.

The Box Model

In descriptive terms, the application of a localised load to the surface of a semi-infinite mass of material causes high vertical compressive stresses in the general region beneath the load. This vertical compression is restrained by the general regions outside the load and near the surface which are therefore in a state of horizontal compression. This behaviour is broadly reproduced by a simple model, the box model, which can easily be analysed exactly. It is illustrated as an inset to fig. 4. For small values of the load P, both inner and outer compartments of the box are in an elastic state. Increasing P produces plastic yielding in the centre compartment while the outer remain elastic. Eventually the outer also yield and the collapse load for the footing is reached. Solutions for the box model for a non-softening purely cohesive material are shown in fig.4. The depth and width of the box have been selected so that the initial elastic slope and the load at which, for an initially unstressed state, local yield first occurs both agree with the known values for an elastic half-space. When scaled to the same collapse load, the solutions from the box model are seen to agree quite well with those by an elasto-plastic finite analysis for the half-space (D'Appolonia et al 1971) even when the initial state of stress is not zero. These finite element solutions can be regarded as accurate enough for this purpose since difficulties of numerical accuracy are not nearly as great for non-softening material as for softening. Thus the box model has promise for semi-quantitative examination of strain-softening and other departures from the properties of the simple ideal elasto-plastic material.

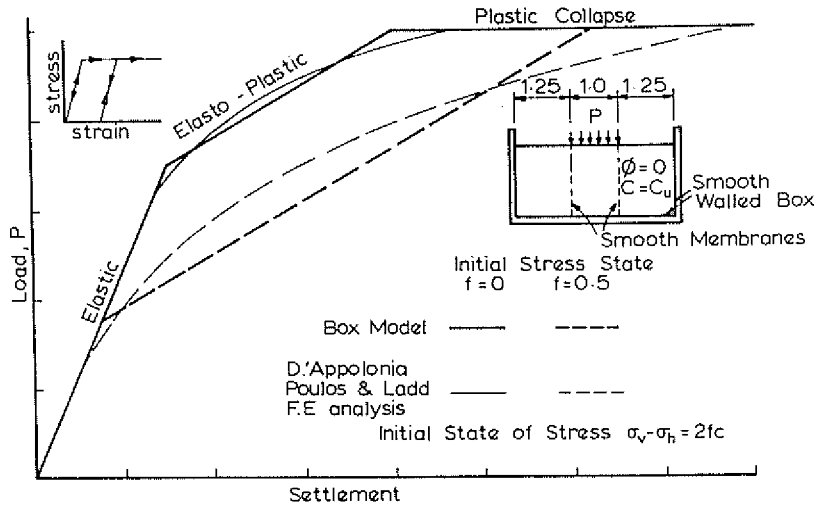

FIG 4 THE BOX MODEL

Solutions from the box model for a purely cohesive material with a low softening ratio (0.02, a value which may be typical of sensitive clays) are shown in fig 5. The peak bearing capacity is only slightly less than that predicted from the peak strength.

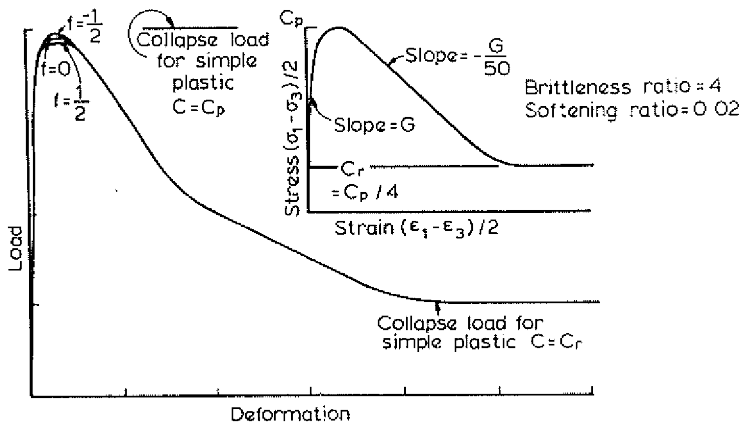

FIG.5 BEARING CAPACITY OF A STRAIN-SOFTENING MATERIAL-LOW SOFTENING RATIO

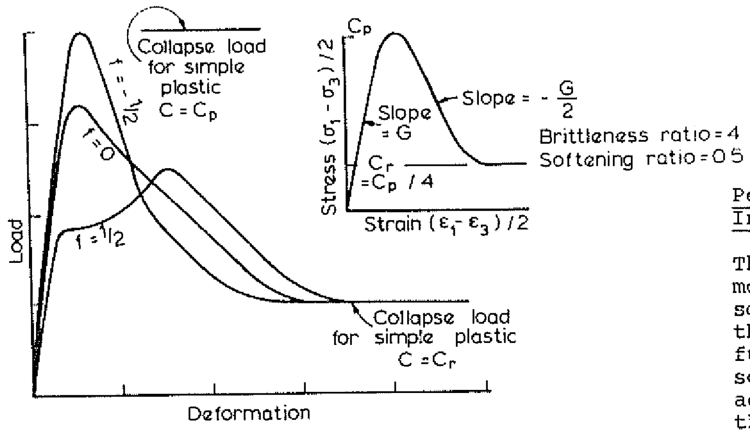

FIG.6 BEARING CAPACITY OF A STRAIN-SOFTENING MATERIAL-HIGH SOFTENING RATIO

(assuming no softening) and is also only slightly affected by the initial stress state. In contrast, fig.6 gives the results for a much more brittle material with a high softening ratio (0.5, perhaps appropriate for a purely cohesive version of a soft rock). This figure shows that in this case the peak bearing capacity may be very significantly less than that predicted from the peak strength (assuming no softening) and that the initial stress has a very marked effect. It can also be remarked that, according to the box model, the ultimate or residual bearing capacity is completely unaffected by the initial state of stress and is that predicted for a simple non-softening material using the residual strength as the constant strength. This can be seen in fig's 5 and 6. Fig.3 also gives some indication that this may be experimentally correct for sands.

For zero initial stress, the effect of increasing softening ratio is shown in fig.7, again using the box model for the analysis. This suggests that beyond a critical softening ratio (point A) further brittleness, that is further increase in the softening ratio causes no further decrease in the peak bearing capacity, and that, even if the residual shear strength approaches zero, the peak bearing capacity of purely cohesive soil does not drop below 50% of the value for the non-softening material. (A more exact analysis than the box model, using the approach discussed in the next section, indicates that the percentage should be about 39 rather than 50.)

Peak Bearing Capacity of Brittle Intact Rock

The indication from the box model that there is a critical softening ratio beyond which the peak bearing capacity is not further reduced by increasing softening ratio, suggests an adaption of simple plasticity theory which has implications for the bearing capacity of intact rock. The analysis for a strip footing is outlined in fig 8. Since, for all but deep or very large foundations, the stresses due to body forces are small compared with the compression strength of most types of rock, such body forces are neglected in the solution given in fig.8. It is assumed that the rock is brittle and therefore has a high softening ratio equivalent in fig.7 to lying along the horizontal line AB. It is further assumed that the softening consisting mainly of the breaking of brittle bonds between rock particles so that the peak strength, as for example measured in unconfined compression tests (q_u), arises from a peak friction angle, ϕ_p and a peak cohesion, c_p; whereas the residual strength is purely frictional with a frictional angle ϕ_r probably less than ϕ_p, the cohesion being destroyed ($c_r = 0$). In fig.8 OABC is a zone where the strains have been sufficient to pass the material to its residual condition - it is the equivalent of the centre compartment of the box model. On the other hand, it is reasonable to assume that the region OCD has only just reached its peak strength when the load reaches its peak bearing capacity value. OCD is the equivalent of the outer compartment of the

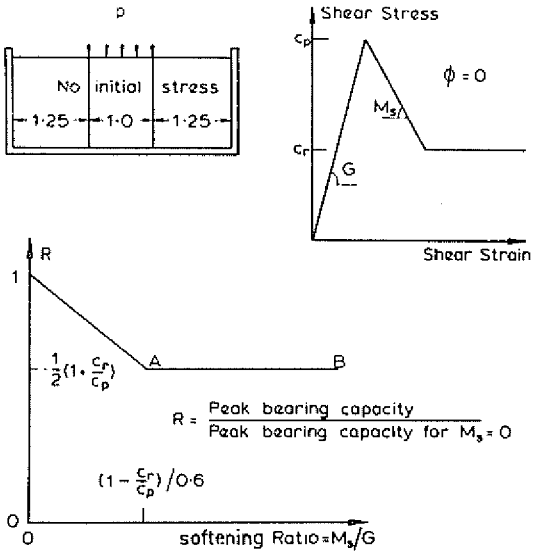

FIG 7 EFFECT OF SOFTENING RATIO ON PEAK BEARING CAPACITY

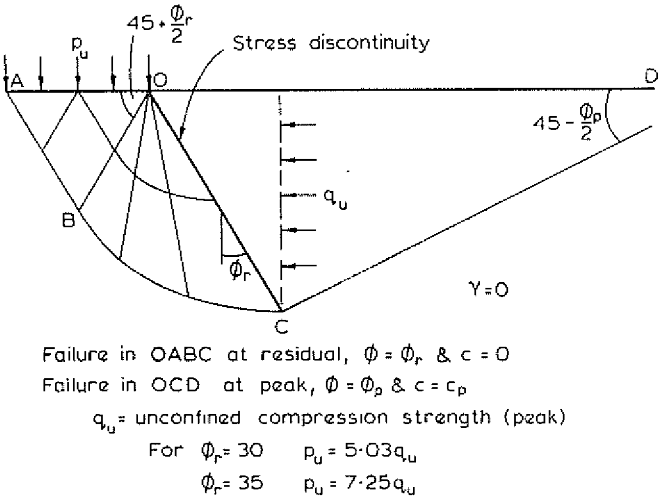

FIG.8 PEAK BEARING CAPACITY OF A BRITTLE INTACT ROCK

FIG.9 ANISOTROPY DUE TO FISSURES OR DEFECTS

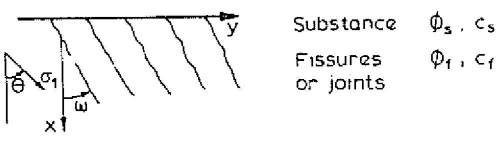

box model. For kinematic and static admissibility OC is a stress and velocity discontinuity and it can be shown that it has to be at ϕ_r to the vertical. The peak bearing capacity only depends on ϕ_r and q_u. ϕ_p and c_p only affect the result insofar as they together determine q_u.

For the reasonable range of 30° to 35° for ϕ_r the peak bearing capacity is predicted to be five to seven times the unconfined compression strength. This agrees well with general experience and is much lower than the value given by the usual Prandtl plasticity solution for a non-softening material having a constant strength represented by ϕ_p and c_p. For example, for the relatively modest plane strain value of ϕ_p = 40°, the Prandtl bearing capacity is nearly 18 times the unconfined compression strength.

Defects

In this section the soil or rock is assumed to be a simple plastic with no strain softening properties but it is assumed that the mass consists of substance material having cohesion c_s and friction angle ϕ_s and containing sets of continuous defects or fissures closely spaced relative to major dimensions of any problem such as the width of a footing, at constant inclinations ω to the vertical and having shear strengths on the defects defined by c_f ($\leq c_s$) and ϕ_f ($\leq \phi_s$). One set of defects is illustrated in fig 9. The combined material, substance plus defects, is equivalent to a special version of a homogeneous plastically anisotropic material. The bearing capacity of purely cohesive soil with an anisotropy which varies smoothly with rotation of the principal directions is dealt with by Davis and Christian (1971) and the more general cohesive-frictional case by Booker and Davis (1972).

For plane strain conditions, the failure surface for an anisotropic material needs to be specified in a three dimensional stress space. It is convenient to select $X=(\sigma_x-\sigma_y)/2$, $Y=(\sigma_x+\sigma_y)/2$ and $Z=\tau_{xy}$ as the cartesian coordinate system. For failure in the substance only, the failure surface will be a cone centred on the Z axis. The circular intersection of this cone with the plane Z=const. is shown as the left-hand diagram of fig.10. For failure on the defects only, the failure surface is a pair of planes which for Z= const., appear as the two straight lines intersecting at $2\phi_f$ as shown in the centre diagram of fig.10. The composite material therefore has a failure surface

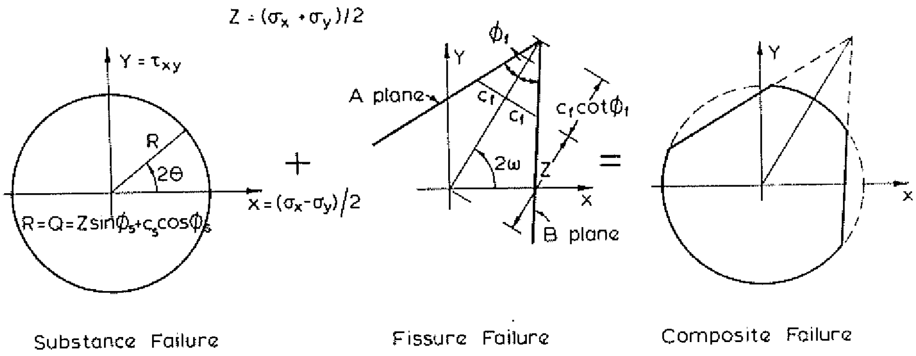

FIG.10 COMPOSITE FAILURE IN PLANE Z=const.

consisting of a cone with flats as indicated by the full lines in the right-hand diagram of fig.10. The plane surfaces for defect failure and the conical surface for substance failure intersect the plane Y=0 in the full lines shown in fig.11.

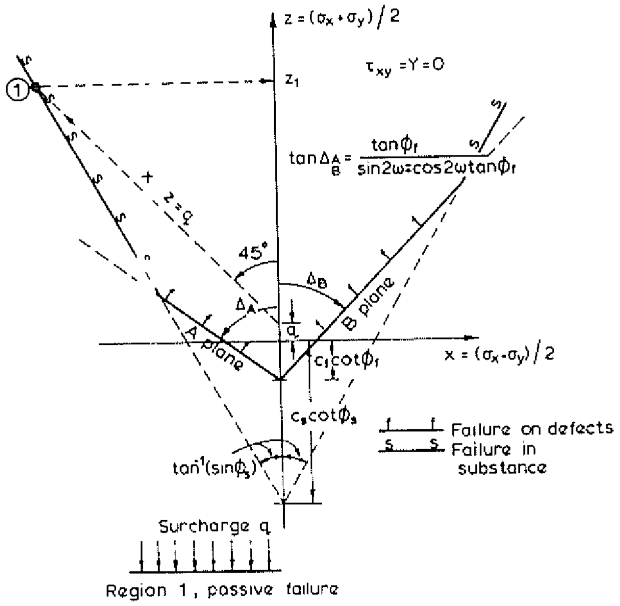

FIG 11 COMPOSITE FAILURE SURFACE IN PLANE Y=0

Fissured Clay

When ϕ=0 the conical failure surface for substance failure becomes a cylinder of radius c_s and the defect failure surfaces become parallel planes $2c_f$ apart. This is illustrated in fig.12a. It can be seen from this figure that the addition of a second set of defects orthogonal to the first causes no change in the failure surface and hence no change to the solution for bearing capacity or any other stability problem.

For purely cohesive material it can be shown (Davis and Christian 1971, and Booker and Davis 1972) that the vertical bearing

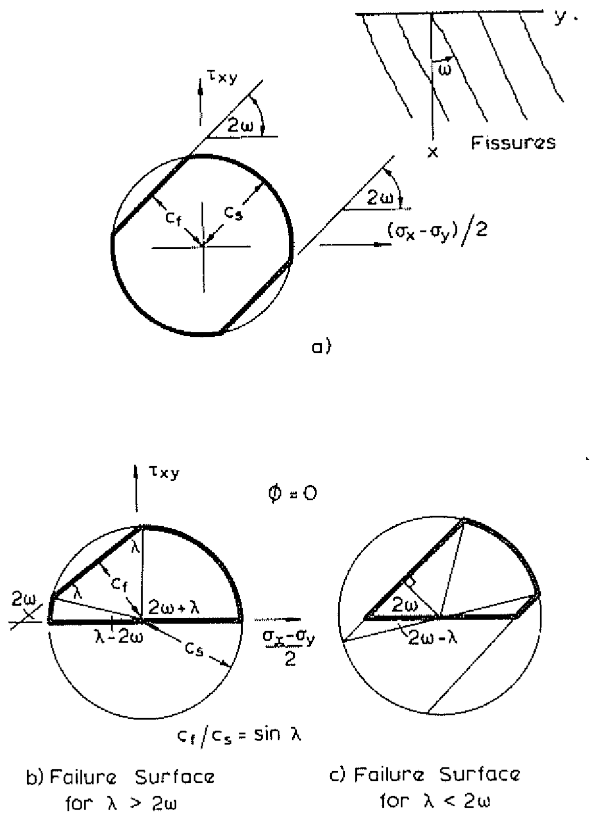

FIG 12 COMPOSITE FAILURE SURFACE FOR ϕ = 0

capacity of a strip footing is given by the length of the solid line in fig's 12b and c. As these figures indicate, two cases arise: $\lambda > 2\omega$ and $\lambda \leq 2\omega$, where $\sin\lambda = c_f/c_s$. The geometry of the figures gives the following equations for the bearing capacity:

$$p_u/c_s = 2(\cos\lambda + \lambda + 1) \quad \text{for } \lambda \geq 2\omega \quad \ldots(1)$$

$$p_u/c_s = 2(\cos\lambda + \lambda + \sin\lambda \text{ cosec } 2\omega) \quad \text{for } \lambda \leq 2\omega \quad \ldots(2)$$

It will be seen that for the first case the inclination of the defects has no influence on the bearing capacity. The solution for multiple sets of defects can easily be obtained in a similar manner.

In the above $0 < \omega < 45^{o}$, but any value of ω outside this range always has an equivalent value within it because ω is equivalent to $90^{o} + \omega$ and is also equivalent to $-\omega$. However, although two sets of defects at ω and $90 + \omega$ give the same bearing capacity as either one on its own, two sets at ω and $-\omega$ give a lower bearing capacity. For example, two sets at 22.5^{o} and -22.5^{o} having the same c_f, or more generally at ω and $\omega - 45^{o}$, give a bearing capacity of $2c_f(2 + \sec 2\omega)$ independent of c_s, provided $c_f/c_s \leq 1/\sqrt{2}$.

The bearing capacity for a single set of defects (or for two orthogonal sets) is plotted in fig.13 from which the very significant potential weakening effect of the defects or fissures in clay can be seen.

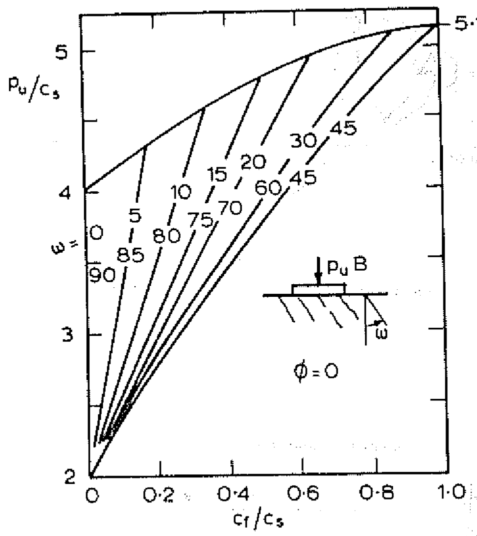

FIG.13 EFFECT OF FISSURE STRENGTH AND ORIENTATION ON VERTICAL BEARING CAPACITY

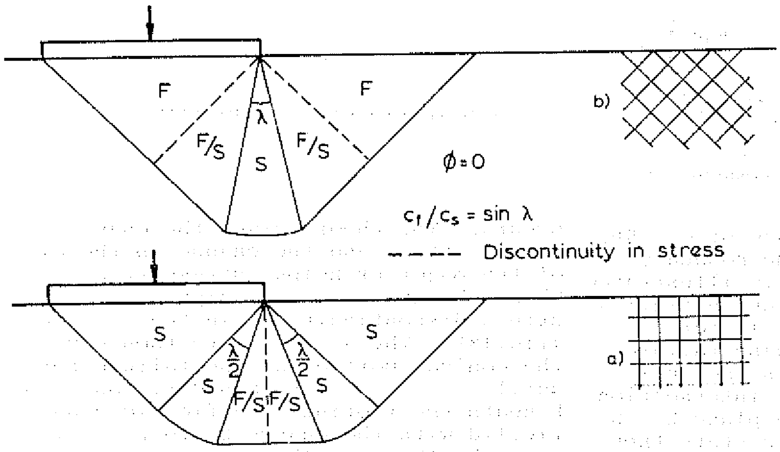

FIG.14 BEARING CAPACITY—SLIP PATTERNS FOR FISSURED CLAY

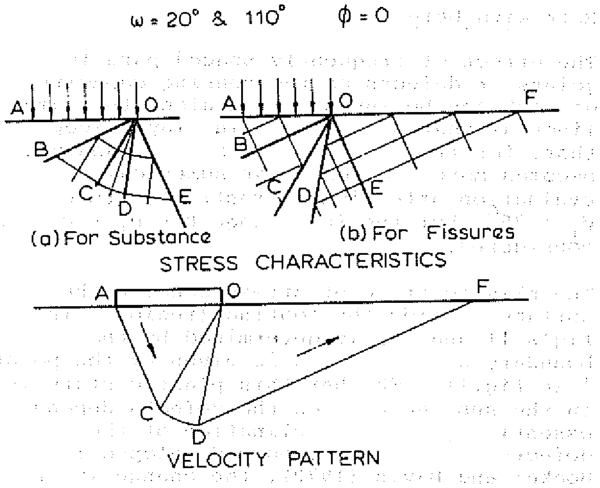

FIG.15 BEARING CAPACITY OF FISSURED CLAY

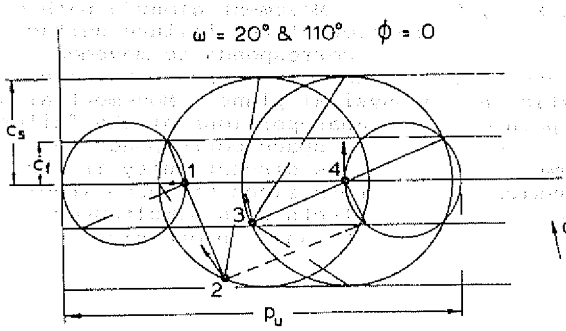

FIG.16 MOHR CIRCLES FOR PROBLEM OF FIG.15

More detail of the solutions is provided by figures 14, 15 and 16. Fig.14a gives the slip patterns for defects at $\omega = 0$ and/or $\omega = 90^{o}$. This figure applies through the range $0 < c_f/c_s < 1$ and the bearing capacity is given by equation 1. (For $c_f/c_s = 0$ equation 2 applies.) Fig 14b is for defects at $\omega=45^{o}$ and/or $\omega= -45^{o}$ and applies for all values of c_f/c. The bearing capacity is given by equation 2. In both cases there is at least one stress discontinuity and there are regions of simultaneous failure in the substance and on defects. It is this which enables the solution to be both kinematically and statically admissible and therefore, by the limit theorems, the exact solution. A more general case, $\omega = 20^{o}$ and/or $\omega = 110^{o}$, is shown in fig 15 for c_f/c_s ratios typified by fig 12c. Again, there are stress discontinuities and regions of simultaneous defect and substance failure. The Mohr circles for this case are shown in fig 16.

Rock with Defects

The effect of frequently spaced parallel joints or defects on the bearing capacity of rock can be investigated along the same lines as that of fissures in clays except that, for frictional material, the analysis becomes more complex. For numerical evaluation attention is restricted to $\phi_s = \phi_f = 35^\circ$ but the full range $0 \leq c_f \leq c_s$ is considered.

The plastic state of stress beneath the surface outside the footing (region 1 in fig's 11 and 18) is determined by the boundary condition and is given by the point 1 in fig.11. Whether this plastic state is in the substance or on the defects depends essentially on the inclination of the defects. Using the theory developed in Booker and Davis (1972), the change in the plastic stress state, in moving along a stress characteristic in the physical plane from region 1 to the region beneath the footing, can be evaluated. This change in stress state is a path on the failure surface in X, Y, Z space. Movement along a path on the conical portion of the failure surface in X, Y, Z space corresponds to movement along a curved substance stress characteristic in the physical plane. Movement along a path on the planar portions of the failure surface in X, Y, Z space corresponds to a jump across a stress discontinuity in the physical plane, both sides of which involve failure on the defects with simultaneous failure in the substance on one side.

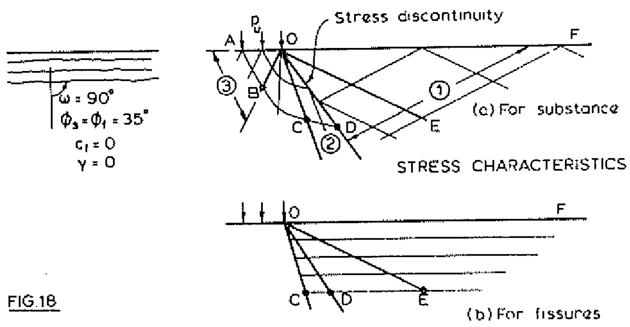

FIG.18

STRESS FIELDS FOR BEARING CAPACITY OF ROCK WITH HORIZONTAL DEFECTS

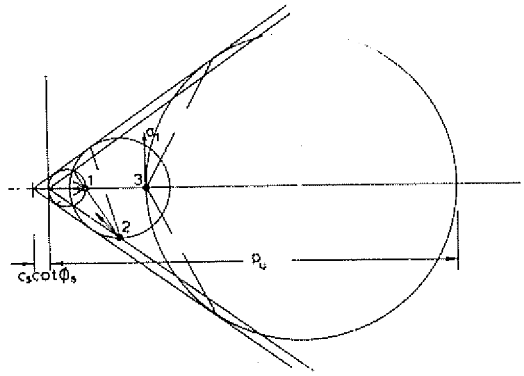

FIG 19 MOHR CIRCLES FOR PROBLEM OF FIG 18

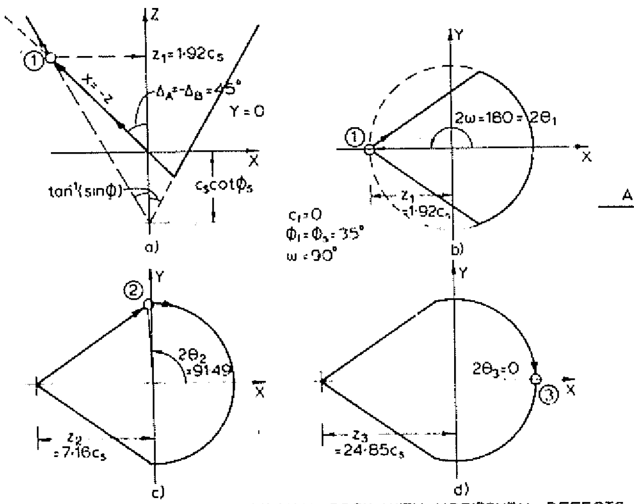

FIG 17 FAILURE SURFACE, FRICTIONAL ROCK WITH HORIZONTAL DEFECTS

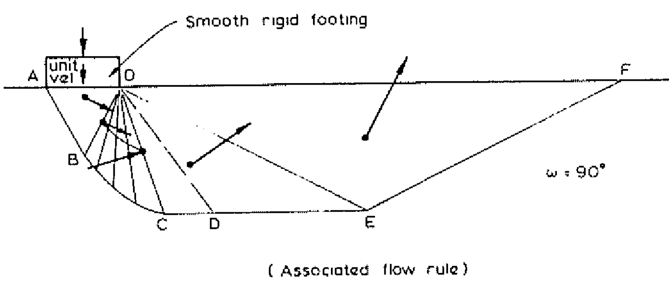

FIG 20 VELOCITY FIELDS FOR PROBLEM OF FIG 18

As an example, consider the case of $\omega = 90$, $c_f = 0$ and surcharge $q = 0$. The boundary condition for region 1, generally illustrated in fig.11, now becomes that given in fig.17a with the value of the stress Z_1 (Z for region 1) indicated. In this case failure in region 1 is simultaneously in the substance and on the defects. The intersection of the failure surface with the plane $Z = Z_1$ is shown in fig.17b. The stress state then moves along a path on the planar portion of the failure surface until at point 2 (fig.17c) simultaneous failure in the substance again occurs. The theory gives the change in Z from Z_1 to Z_2 and the change in the direction of the major principal stress from θ_1 to θ_2. These changes occur as jumps across the stress discontinuity OD in the physical plane (fig.18). The stress state then moves over the conical portion of the failure surface until $\theta = \theta_3 = 0$ (the boundary condition beneath the footing) and fig.17c changes to fig.17d with the change Z_1 to Z_2 evaluated from the theory. This change in stress state from (2) to (3) corresponds to the centred fan BOC in fig.18. The bearing capacity p_u

can be readily calculated from Z_3. The Mohr circles for the stress states (1), (2) and (3) are given in fig.19 and the velocity pattern, assuming an associated flow rule, is given in fig.20.

For values of ω other than 90°, the solutions also always have at least one discontinuity and have regions of simultaneous defect and substance failure, but the sequence of regions may be different and the number of regions greater. They can become considerably more complex.

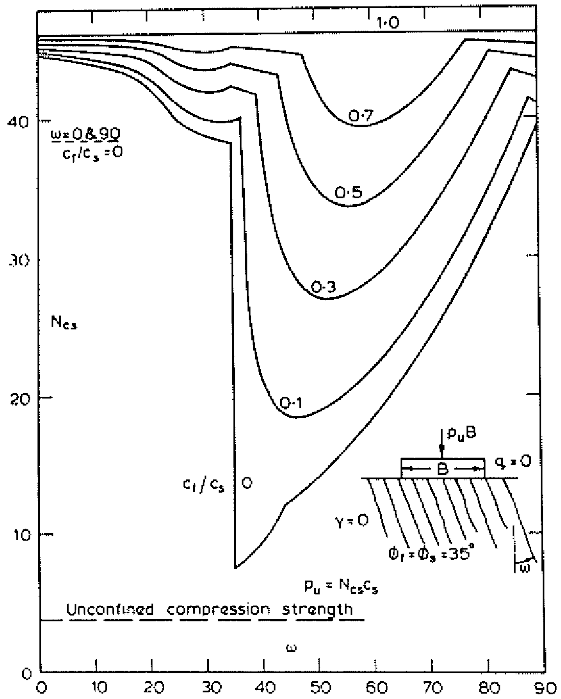

FIG 21 EFFECT OF DEFECT ORIENTATION ON BEARING CAPACITY OF ROCK

The results of the analysis for the full range of c_f/c_s and ω are given in fig.21. The horizontal line for $c_f/c_s = 1$ at the top of the figure gives the bearing capacity without any weakening from defects. For comparison, the unconfined compression strength is also shown at the bottom of the figure. It can be seen that for low values of ω the defects do not cause a very large loss of bearing capacity, and similarly for ω close to 90°, but that in between the loss can be very great. The vertical drop for $\omega = \phi = 35^{\circ}$ when $c_f/c_s = 0$ arises from the fact that no force can be applied to a purely frictional interface if the angle of obliquity is greater than the friction angle but that the force is unlimited if the angle of obliquity is even infinitesimally less than the friction angle. The other kinks in the curves arise from changes in the mode or sequence of plastic regions in the solutions.

The results of fig.21 apply equally well to negative values of ω. The effect of more than one set of defects has not been studied in any detail but there are no theoretical difficulties to such extension. In general, every additional set will cause further lowering of the bearing capacity although not necessarily to a great extent. For example, the solution for the two sets $\omega = 0$ and 90°, with $c_f/c_s = 0$, is indicated in fig.21, and gives a value only slightly below that for the single set $\omega = 90^{\circ}$.

The results of fig.21 are for zero surcharge but, by the following transformation, the effect of surcharge can be included.

Let the required case be:

$\phi_s = \phi_f = \phi$ (= 35°)

defect cohesion $= c_{fa}$

substance cohesion $= c_{sa}$

surcharge $= q$

Then bearing capacity:

$$p_u = N_{cs} (c_{sa} + q \tan\phi) + q$$

where N_{cs} is the value from fig.21

for $$\frac{c_f}{c_s} = \frac{c_{fa} + q \tan\phi}{c_{sa} + q \tan\phi}$$

Conclusion

It is hoped that the examples given in this lecture demonstrate that plasticity theory is capable not only of dealing with a very simple ideal material (so removed from real materials that it is suspected by many of being of little practical value), but is capable of giving insight into the effects of such aspects of real soil and rock as its semi-brittle or strain softening behaviour and the existence of joints, fissures and other defects. The theory shows that both can reduce the load capacity of a mass of soil or rock very considerably - a conclusion giving satisfactory confirmation of common sense!

Acknowledgement

The value of discussions with Dr J.R. Booker, of many aspects of the theoretical analyses from which the results given in this lecture were derived, is gratefully acknowledged.

References

ABOUSTIT, B.L. and D.V. REDDY (1980)
Finite element linear programming approach to foundation shakedown Proceedings International Symposium, Soils under cyclic and transient loading, Swansea

BOOKER, J.R. and E.H. DAVIS (1972)
A general treatment of plastic anisotropy under conditions of plane strain J. Mech. Phys. Solids, Vol 20.

D'APOLONIA, D.J. H.G. POULOS and C.C. LADD (1971)
Initial settlement of structures on clay J. S.M. and F. Div., ASCE; Vol 97, No SM10.

DAVIS, E.H. and J.R. BOOKER (1971)
The bearing capacity of strip footings from the standpoint of plasticity theory Proceedings 1st Australian/New Zealand Conference on Geomechanics

DAVIS. E.H. and J.T. CHRISTIAN (1971)
Bearing capacity of anisotropic cohesive soil J. S.M. and F. Div., ASCE; Vol 97, No SM5

KIRKPATRICK, W.M. (1977)
Private communication

PANDE, G.N., W.S. ABDULLAH and E.H. DAVIS (1980)
Shakedown of elasto-plastic continua with special reference to soil/rock structures Proceedings International Symposium Soils under cyclic and transient loading, Swansea.

SWANE, I.C. (1980)
Private communication